

Effective masses in a strongly anisotropic Fermi liquid

Tudor D. Stanescu,¹ Victor Galitski,¹ and H. D. Drew²

¹*Department of Physics and Joint Quantum Institute, University of Maryland, College Park, MD 20742-4111*

²*CNAM, University of Maryland, College Park, MD 20742-4111*

Motivated by the recent experimental observation of quantum oscillations in the underdoped cuprates, we study the cyclotron and infrared Hall effective masses in an anisotropic Fermi liquid characterized by an angle-dependent quasiparticle residue Z_q , which models an arc-shaped Fermi surface. Our primary motivation is to explain the relatively large value of the cyclotron effective mass observed experimentally and its relation with the effective Hall mass. In the framework of a phenomenological model of an anisotropic Fermi liquid, we find that the cyclotron mass is enhanced by a factor $\langle 1/Z_q \rangle$, while the effective Hall mass is proportional to $\langle Z_q \rangle / \langle Z_q^2 \rangle$, where $\langle \dots \rangle$ implies an averaging over the Fermi surface. We conclude that if the Z -factor becomes small in some part of the Fermi surface (e.g., in the case of a Fermi arc), the cyclotron mass is enhanced sharply while the infrared Hall mass may remain small. Possible future experiments are discussed.

PACS numbers: 71.10.-w, 71.10.Ay, 74.72.-h

Recently, the observation of magnetic quantum oscillations was reported in YBCO single crystals [1, 2, 3, 4] (ortho-II $\text{YBa}_2\text{Cu}_3\text{O}_{6.5}$ and $\text{YBa}_2\text{Cu}_4\text{O}_8$) with periods in $1/H$ indicative of small Fermi surface (FS) pockets (area $\sim 2.4\%$ of the Brillouin zone). These materials are examples of hole doped cuprates in the pseudogap region of the phase diagram where the ubiquitous anomalous physical properties have attracted much attention. ARPES measurements [5, 6], for example, have revealed that portions of the full Fermi surface observed in optimally doped and overdoped cuprates are obliterated in the pseudogap phase, leaving behind so-called Fermi arcs. However these ARPES Fermi arcs are not closed surfaces and how they could figure into the quantum oscillations is the subject of much current discussion. The magnetic quantum oscillations experiments probe the geometry of the Fermi surface and the quasiparticle dynamics in these strongly correlated systems. The exotic properties of these materials are widely believed to be tied to the competition between strong fluctuations associated with magnetic, charge and superconducting order, occurring close to a magnetically ordered Mott state. Interactions with these fluctuations also govern the quasiparticle dynamics.

One surprising result in the experiments is that the observed cyclotron frequencies, $\omega_C = eB/(m_C c)$, seem quite small for the size of the pockets. The cyclotron frequency measured by the damping of the quantum oscillations is the inverse time for the quasiparticles to traverse a closed complete orbit around the Fermi surface. The observed cyclotron masses, m_C , are comparable with the quasiparticle masses estimated for the full unreconstructed FS (area $\sim 70\%$ of the Brillouin zone) of optimally doped cuprates obtained from ARPES and other experiments. On very general grounds m_C is expected to scale with the pocket size as $m_C \sim \Delta k/v_F$, where the Fermi pocket area is $\sim \Delta k^2$ and v_F is the Fermi velocity which can be measured directly by ARPES. Therefore, developing an understanding of the value of m_C observed in experiment is important to understanding the interactions in the pseudogap phase.

Other experimental probes measure characteristic masses which depend differently on the k -dependent dynamical mass tensor on the FS. ARPES measures the k -dependent quasiparticle dispersion from which m_k can be estimated. Specific heat, optics and magneto transport measurements also produce masses which correspond to different averages of the k -dependent mass on and near the Fermi surface. In particular the Hall Effect performed at infrared (IR) frequencies [7, 8, 9, 10, 11] is characterized by a Hall mass, m_H . Experiments measuring this quantity in several hole doped cuprates have revealed that m_H , which is comparable to the ARPES masses in optimally doped materials, decreases rapidly in underdoped cuprates as expected from the above argument. It is surprising, however, that the values of the Hall and cyclotron masses appear to violate the relation $m_H \geq m_C$, which occurs for models of simple convex Fermi surfaces for weakly-interacting quasiparticles. For example, if m_1 and m_2 are the components of the mass tensor characterizing an elliptical FS, $m_C = \sqrt{m_1 m_2}$ can be significantly smaller than $m_H = (m_1 + m_2)/2$ for an elongated pocket.

In this paper we propose an explanation for the behavior of the effective masses based on a model of a highly renormalized Fermi liquid characterized by a reconstructed FS and strongly momentum-dependent quasiparticle properties. The existence of a reconstructed FS in the underdoped cuprates is suggested by the observation of quantum oscillations, as well as by ARPES and IR Hall measurements. Whether this reconstructed FS consists of closed Fermi pockets or disconnected Fermi arcs is still a matter of debate. In this work we assume that the first possibility is realized and we study the implications for the behavior of the effective masses. One scenario that could lead to a FS reconstruction involves some type of order, such as antiferromagnetism [12], d-density wave [13], or stripe[14] order, present in the system. Another possibility is that the reconstruction is due to the strong electron correlations generated by the proximity to a Mott phase [15, 16, 17]. In this scenario the formation of small Fermi pockets is the

result of strong finite range correlations and no broken symmetry needs to be invoked. Moreover this scenario does not require energy gaps in the quasiparticle dispersion relations, in contrast to the broken symmetry phases, which is consistent with the experimental observations of optics, IR Hall and ARPES measurements. While this scenario does not exclude the existence of broken symmetry phases at low temperatures [17], it emphasizes the key role of competing short-range correlations in the physics of the underlying “normal” state. At a formal level, the FS reconstruction is the consequence of a large, strongly momentum-dependent self-energy [15]. The self-energy effects lead to a k -dependent low-energy physics having two major characteristics: 1) Fermi liquid-like quasiparticles exist along a reconstructed FS that shrinks as doping is reduced, while a (pseudo)-gap opens in other regions of the Brillouin zone. 2) The properties of the quasiparticles along the reconstructed FS are highly anisotropic. Consequently, physical quantities describing the quasiparticle are momentum-dependent and contribute to experimentally measured quantities through specific averages over the FS. It is therefore natural to address the following questions: What is the experimental signature of a highly anisotropic Fermi liquid? In particular, what is the effect of the anisotropy on the effective masses extracted from various measurements?

To address these questions we study a phenomenological model of an anisotropic Fermi liquid, which mimics the arc-shaped Fermi pockets and may lead to the experimentally observed quantum oscillations. We are not concerned here with the physical mechanism responsible for the existence of these pockets. Our main assumption is that the low-energy physics is determined by quasiparticles with highly anisotropic properties. Moreover, we focus on the effects of an anisotropic self-energy that produces a strongly angle-dependent quasiparticle residue $Z_{\mathbf{q}}$. Our starting point is the Fermi-liquid Green function

$$G(\omega, \mathbf{q}) = \frac{1}{\omega(1 + \alpha_{\mathbf{q}}) - \xi_{\mathbf{q}} + i\eta} \quad (1)$$

where $\xi_{\mathbf{q}} = (q_1^2/2m_1 + q_2^2/2m_2) - \epsilon_F$, with ϵ_F being the Fermi energy) represents a parabolic bare band characterized by a two-dimensional elliptic Fermi surface. The anisotropy along the Fermi surface is determined by the momentum-dependent self-energy $\Sigma(\omega, \mathbf{q}) = -\omega\alpha_{\mathbf{q}} - i\eta$. A particular choice of the anisotropy parameter $\alpha_{\mathbf{q}}$ is discussed below. Note that the quasiparticle residue $Z_{\mathbf{q}} = (1 + \alpha_{\mathbf{q}})^{-1}$ represents the spectral weight of the quasiparticle peak in the spectral function. Consequently, in the presence of a large anisotropy, the low-energy spectral weight associated with the Fermi surface will have an arc-like shape (see Fig. 1). We assume that the ω^2 momentum-dependent contribution to the imaginary part of the self-energy is negligible in the relevant frequency range. In addition, we make the assumption that frequency-independent contribution ($-i\eta$) is weakly momentum-dependent and we consider it a constant. In general, the effects of the quasiparticle residue anisotropy, $Z_{\mathbf{q}} = (1 + \alpha_{\mathbf{q}})^{-1}$, and those determined by the scattering time

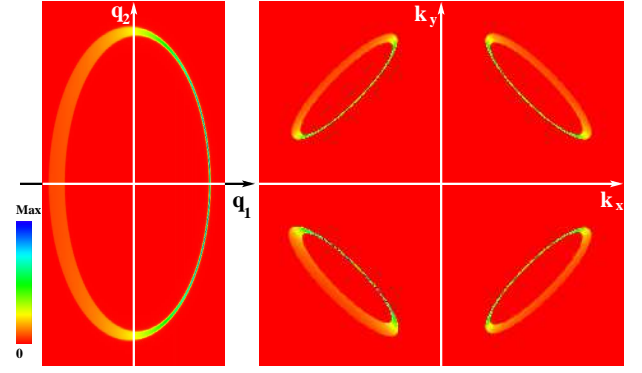


FIG. 1: (Color online): Spectral weight at the Fermi energy for a Fermi pocket described by the Eq. (1) with $m_2 = 4m_1$ and $\alpha_{\mathbf{q}} = 5(q_1/q_F^{(1)} - 1)^2$ (left). The spectral weight is obtained by integrating $A(\omega, \mathbf{q}) = -\text{Im}G(\omega, \mathbf{q})/\pi$ over a small frequency window about the Fermi energy. The right panel shows a symmetric distribution of Fermi pockets in momentum space.

anisotropy, $1/2\tau_{\mathbf{q}} = \eta_{\mathbf{q}}$ are entangled, but we will operate under these simplifying conditions in order to clearly identify the relevant effects. Note that Eq. (1) describes one Fermi pocket in a properly chosen coordinate system. When calculating physical observables, we need to restore the symmetry by averaging over several pockets symmetrically arranged in momentum space (see Fig. 1).

We now consider a two-dimensional system described by Eq. (1) in the presence of a uniform magnetic field \mathbf{B} oriented along the direction perpendicular to the two-dimensional plane. The effects of the magnetic field are introduced, based on the work by Luttinger [18] and Roth [19], through the standard substitution $\mathbf{q} \rightarrow -i\nabla - \frac{e}{c}\mathbf{A}$ made both in the bare band $\xi(\mathbf{q})$ and the self-energy [20]. Consequently, the anisotropy of the quasiparticle residue has a direct impact on the effective Landau level structure. In the presence of the magnetic field, the system is described by the operator $\hat{G}_\omega = [\omega - \hat{K}_\omega + i\eta]^{-1}$, where $\hat{K}_\omega = \xi(-i\nabla - \frac{e}{c}\mathbf{A}) - \omega\alpha(-i\nabla - \frac{e}{c}\mathbf{A})$. The next step is to find the eigenvalues of the operator \hat{K}_ω for each frequency. In order to make this step mathematically tractable, we make the following explicit choice for the momentum dependence of the anisotropy factor (consistent with the arc-shaped form of a pocket) $\alpha_{\mathbf{q}} = \alpha\left(\frac{q_1}{q_F^{(1)}} - 1\right)^2$, where α is a positive number and $q_F^{(1)} = \sqrt{2m_1}\epsilon_F$ is the Fermi k -vector along the direction “1”. With this choice, the quasiparticle strength is continuously reduced from $Z_{(q_F^{(1)}, 0)} = 1$ on one side of the Fermi pocket to $Z_{(-q_F^{(1)}, 0)} = 1/(1 + 4\alpha)$ on the opposite side. Writing the vector potential in the symmetric gauge as $\mathbf{A} = \left(-\frac{B}{2}x_2, \frac{B}{2}x_1\right)$, the operator \hat{K}_ω becomes

$$\hat{K}_\omega = \frac{(-i\partial_{x_1} + \frac{eB}{2c}x_2)^2}{2m_1} + \frac{(-i\partial_{x_2} - \frac{eB}{2c}x_1)^2}{2m_2} - \frac{\alpha\omega}{(q_F^{(1)})^2} \left(-i\partial_{x_1} + \frac{eB}{2c}x_2 - q_F^{(1)}\right)^2 - \epsilon_F. \quad (2)$$

The eigenproblem for this operator can be reduced to the standard Landau-level problem by first separating a plane-wave factor $\exp[-ix_1 q_F^{(1)} \alpha \omega / (\epsilon_F - \alpha \omega)]$ in the eigenfunction, then rescaling the variables $x_1 \rightarrow \tilde{x}_1 \lambda$, $x_2 \rightarrow \tilde{x}_2 / \lambda$ with $\lambda = (m_2/m_1)^{1/4} (1 - \alpha \omega / \epsilon_F)^{1/4}$. The corresponding ‘‘Landau levels’’ are

$$W_n(\omega) = \omega_C \sqrt{1 - \frac{\alpha \omega}{\epsilon_F}} \left(n + \frac{1}{2} \right) - \frac{\alpha \omega}{1 - \frac{\alpha \omega}{\epsilon_F}} - \epsilon_F, \quad (3)$$

where $\omega_C = eB/c \sqrt{m_1 m_2}$ represents the cyclotron frequency of the elliptic pocket in the absence of the self-energy anisotropy. Finally, we identify the physical Landau levels, i.e., we determine the frequencies at which the Green function has poles, by solving the equation $\omega - W_n(\omega) = 0$. Focusing on the relevant low-frequency regime, $\alpha \omega \ll \epsilon_F$, we obtain the set of solutions $\omega_j = \frac{\omega_C}{c} j + \delta / (1 + \frac{3}{2} \alpha)$, with $j = 0, \pm 1, \pm 2, \dots$ and $0 \leq \delta < 1$. The effective cyclotron frequency for our model is $\omega_C^* = \omega_C / (1 + \frac{3}{2} \alpha)$ and represents the spacing between Landau levels in the vicinity of Fermi energy. This spacing determines the temperature-dependent damping of the amplitude of quantum oscillations through the standard Lifshitz-Kosevich formula. Consequently, the effective cyclotron mass extracted from an analysis of the temperature dependence of the amplitude of quantum oscillations is $m_C^* = \sqrt{m_1 m_2} (1 + \frac{3}{2} \alpha)$. Note that the enhancement factor of the effective mass due to self-energy effects is exactly $(1 + \frac{3}{2} \alpha) = \langle 1/Z_{\mathbf{q}} \rangle$, where $\langle \dots \rangle$ represents an average over the Fermi surface, and we have

$$m_C^* = \sqrt{m_1 m_2} \left\langle \frac{1}{Z_{\mathbf{q}}} \right\rangle. \quad (4)$$

The cyclotron mass is enhanced by a factor equal to the average of $1/Z_{\mathbf{q}}$ over the Fermi surface. Note that, the quantum oscillations are observable if the quasiparticles have a finite weight everywhere along a closed Fermi surface, as expected from the semi-classical picture. If the $Z_{\mathbf{q}}$ anisotropy is large, the main contribution to the mass comes from the regions with small quasiparticle residue. We note that, within our model, a similar enhancement obtains for the effective thermodynamic mass extracted from the specific heat, $m^* \sim C/T$, and we get $m^* = m_C^*$.

Let us turn now our attention to the evaluation of the longitudinal and Hall dynamical conductivities for the anisotropic Fermi liquid described by Eq. (1). We neglect contributions coming from the current vertex corrections and focus on a frequency regime characterized by $\omega_C \ll \omega$, $1/\tau \ll \epsilon_F$ with $\omega \tau$ arbitrary, where the cyclotron frequency ω_C is the smallest energy scale in the problem and $1/\tau = \eta$ is the inverse scattering time. We also assume a symmetric arrangement of the Fermi pockets (see Fig. 1), so the final values for the conductivities represent averages over the possible orientations. Using the standard Kubo formalism we have

$$\sigma_{\alpha\alpha}(\omega) = \frac{-ie^2}{\omega} T \sum_{\epsilon_n} \sum_{\mathbf{q}} \frac{q_\alpha^2}{m_\alpha^2} G_n(\mathbf{q}) G_{n-}(\mathbf{q}), \quad (5)$$

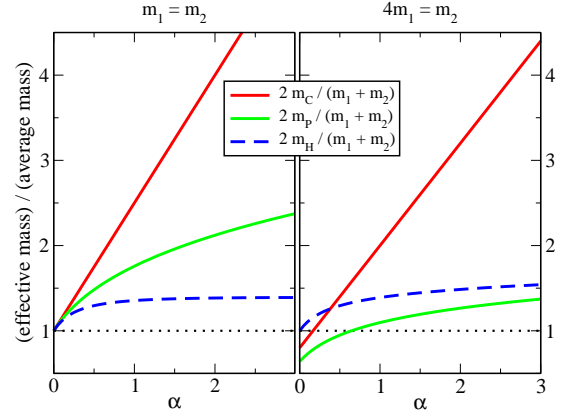


FIG. 2: (Color online): Dependence of the effective masses on the anisotropy of the Fermi surface. The left and right panels correspond to circular and elliptical Fermi surfaces, respectively. The effective cyclotron, plasma and Hall effective masses are calculated using equations (4), (8) and (9). The thermodynamic effective mass extracted from the specific heat coincides with m_C .

$$\sigma_{\alpha\beta}(\omega) = \frac{\pm e^2 \omega_C}{\omega} T \sum_{\epsilon_n, \mathbf{q}} \frac{q_\alpha}{\sqrt{m_1 m_2}} [G_n \partial_\alpha G_{n-} - \partial_\alpha G_n G_{n-}],$$

where we use the notation $G_n \equiv G(i\epsilon_n, \mathbf{q}) = [i\epsilon_n(1 + \alpha_{\mathbf{q}}) - \xi_{\mathbf{q}} + i \text{sign}(\epsilon_n)/(2\tau)]^{-1}$ for the Matsubara Green function, $G_{n-} = G(i\epsilon_n - i\omega_m, \mathbf{q})$, $\partial_\alpha = \partial/\partial q_\alpha$ and $\alpha \neq \beta$. Here, the analytical continuation to real frequencies, $i\omega_m \rightarrow \omega - i\delta$ is implicitly assumed. When performing the sum over \mathbf{q} in (5), it is convenient to rescale the momentum in order to have a circular Fermi surface. We define $\tilde{q}_1 = \sqrt{m_2/m_1} q_1$ and $\tilde{q}_2 = \sqrt{m_1/m_2} q_2$, as well as the angle $\varphi_{\tilde{\mathbf{q}}}$ between the vector $\tilde{\mathbf{q}}$ and the ‘‘1’’-axis. With these notations, the expression of the longitudinal conductivity becomes

$$\sigma_{xx} = \frac{ne^2}{\sqrt{m_1 m_2}} \left\langle \frac{\sqrt{\frac{m_2}{m_1}} \cos^2 \varphi_{\tilde{\mathbf{q}}} + \sqrt{\frac{m_1}{m_2}} \sin^2 \varphi_{\tilde{\mathbf{q}}}}{\frac{1}{\tau} - i\omega(1 + \alpha_{\tilde{\mathbf{q}}})} \right\rangle, \quad (6)$$

where n is the carrier concentration and $\langle \dots \rangle$ represents the average over the (circular) Fermi surface. Similarly, for the Hall conductivity we have

$$\sigma_{xy} = \frac{ne^2}{\sqrt{m_1 m_2}} \omega_C \left\langle \frac{1}{\left[\frac{1}{\tau} - i\omega(1 + \alpha_{\tilde{\mathbf{q}}}) \right]^2} \right\rangle, \quad (7)$$

with $\omega_C = eB/c \sqrt{m_1 m_2}$ being the bare cyclotron frequency. Note that in Eqns. (6) and (7) no assumption has been made about the momentum dependence of the anisotropy factor $\alpha_{\mathbf{q}}$. Also note that similar expressions can be written in the more general case of a momentum-dependent scattering time $\tau_{\mathbf{q}}$. In practice the momentum dependence of τ and also its frequency dependence have to be taken into account. One can see from equations (6) and (7) that any quantity extracted from the low-frequency dynamical conductivities will contain the combined effect of anisotropic $Z_{\mathbf{q}}$ and $\tau_{\mathbf{q}}$.

An interesting and experimentally important regime [7, 8, 9, 10, 11] corresponds to infrared frequencies satisfying $\omega\tau \gg 1$. In this case, τ becomes irrelevant and the leading contribution to the longitudinal conductivity takes the standard form $\sigma_{xx} \approx i\omega_p^2/(4\pi\omega)$, where $\omega_p^2 = 4\pi ne^2/m_p^*$ is the plasma frequency with

$$m_p^* = \frac{\sqrt{m_1 m_2}}{\left\langle \left(\sqrt{\frac{m_2}{m_1}} \cos^2 \varphi_{\mathbf{q}} + \sqrt{\frac{m_1}{m_2}} \sin^2 \varphi_{\mathbf{q}} \right) Z_{\mathbf{q}} \right\rangle}, \quad (8)$$

Note that the plasma frequency defined here includes only contributions coming from low-energy quasiparticles in the vicinity of the Fermi energy. Our phenomenological model does not include incoherent self-energy contributions that should be present in a strongly correlated system above a certain energy scale. In discussing the high-frequency limit we implicitly assume that ω does not exceed that energy scale. The leading high-frequency contribution to the Hall conductivity is $\sigma_{xy} \approx -\omega_p^2 \omega_H / (4\pi\omega^2)$ with $\omega_H = eB/(cm_H^*)$ being the Hall frequency. The corresponding effective mass is

$$m_H^* = \frac{m_1 m_2}{m_p^* \langle Z_{\mathbf{q}}^2 \rangle}. \quad (9)$$

For $Z_{\mathbf{q}} = 1$, Eq. (9) takes the standard form $m_H = (m_1 + m_2)/2$. We note that Eqs. (8) and (9) for the effective masses were obtained without making any assumption about the q -dependence of the anisotropy factor $\alpha_{\mathbf{q}}$ and, implicitly, about the q -dependence of $Z_{\mathbf{q}}$. In addition, as in the case of the cyclotron mass, it is straightforward to show that the same expressions for the effective masses can be obtained for a quasiparticle residue of the form $Z_{\mathbf{q}} = Z_0/(1 + \alpha_{\mathbf{q}})$.

To analyze these results, let us consider, for simplicity, the case of a circular Fermi pocket. The effective cyclotron mass is enhanced by a factor $\langle 1/Z_{\mathbf{q}} \rangle$, while the effective plasma mass is increased by $1/\langle Z_{\mathbf{q}} \rangle$ and the Hall mass by $\langle Z_{\mathbf{q}} \rangle / \langle Z_{\mathbf{q}}^2 \rangle$. In the isotropic case, all these enhancement factors are equal to $1/Z$. However, in the presence of an anisotropy, m_C is enhanced more strongly, due to the singular nature of $1/Z_{\mathbf{q}}$. In contrast, both $1/\langle Z_{\mathbf{q}} \rangle$ and $1/\langle Z_{\mathbf{q}}^2 \rangle$ remain relatively small even for $Z_{\mathbf{q}}$ vanishing at certain q -vectors along the Fermi surface. Consequently, the effective masses extracted from conductivity measurements will be finite even for a Fermi surface consisting in disconnected Fermi arcs. The dependence of the effective masses on the anisotropy factor for $\alpha_{\mathbf{q}} = \alpha (q_1/q_F^{(1)} - 1)^2$ is shown in Fig. 2. The left panel corresponds to a circular Fermi pocket, while the right panel corresponds to the elliptic case. Note that for an elongated Fermi pocket, in the absence of anisotropy, the Hall mass is always larger than the cyclotron mass. However, even a small anisotropy can make m_C^* comparable with or larger than m_H^* .

In conclusion, we have shown that various experimentally relevant effective masses represent different averages over the Fermi surface. The basic ingredients that contribute to the effective mass are the band structure, which determines the bare mass tensor (i.e., the values of m_1 and m_2 in our model),

and the self-energy contributions, which are contained in the quasiparticle residue $Z_{\mathbf{q}}$. It is convenient to regard $Z_{\mathbf{q}}$ as a product of a q -independent factor Z_0 and a momentum-dependent anisotropy factor $1/(1 + \alpha_{\mathbf{q}})$. The main message of this letter is that the $Z_{\mathbf{q}}$ anisotropy plays a key role in establishing the value of a given effective mass. The question concerning the dependence of the anisotropy on doping is beyond the scope of this study. However, we point out that the different components contributing to the effective mass may have a doping evolution with competing effects. For example, as the doping is reduced, the pockets are expected to shrink, leading to a decrease in the bare mass. On the other hand Z_0 , the ‘‘nodal’’ quasiparticle residue, should decrease when approaching the Mott insulator, leading to an enhancement of the effective mass. What about the $Z_{\mathbf{q}}$ anisotropy? If pocket formation is associated with antiferromagnetic fluctuations [21], for example, we can speculate that the anisotropy should be weak at very small doping and increase strongly as we approach optimal doping. In this case, our analysis would predict a very sharp increase of the cyclotron mass upon approaching optimal doping.

A high priority suggested by these considerations is experiments that include a systematic analysis of the cyclotron and Hall effective masses and specific heat as a function of doping in a single material under similar conditions i.e., high magnetic fields and low temperatures. Comparison of these masses with our theoretical predictions will help to determine the relation between the quantum oscillations and the Fermi arcs observed in ARPES and thereby lead to an understanding of the pseudogap in the underdoped cuprates.

H. D. Drew was supported by NSF grant DMR-0303112.

-
- [1] N. Doiron-Leyraud, C. Proust, D. LeBoeuf, J. Levalois, J.-B. Bonnemaison, R. Liang, D. Bonn, W. Hardy, and L. Taillefer, *Nature* **447**, 565 (2007).
 - [2] A. F. Bangura, J. D. Fletcher, A. Carrington, J. Levallois, M. Nardone, B. Vignolle, P. J. Heard, N. Doiron-Leyraud, D. LeBoeuf, L. Taillefer, et al., arXiv:0707.4461 (2007).
 - [3] E. A. Yelland, J. Singleton, C. H. Mielke, N. Harrison, F. F. Balakirev, B. Dabrowski, and J. R. Cooper, *Phys. Rev. Lett.* **100**, 047003 (2008).
 - [4] C. Jaudet, D. Vignolles, A. Audouard, J. Levallois, D. LeBoeuf, N. Doiron-Leyraud, B. Vignolle, M. Nardone, A. Zitouni, R. Liang, et al., arXiv:0711.3559 (2007).
 - [5] A. Damascelli, Z. Hussain, and Z.-X. Shen, *Rev. Mod. Phys.* **75**, 473 (2003).
 - [6] K. Shen, F. Ronning, D. Lu, N. Ingel, W. Lee, W. Meevasana, F. Baumberger, T. Kohsaka, M. Azuma, M. Takano, et al., *Science* **307**, 901 (2005).
 - [7] Y. Dagan, M. M. Qazilbash, C. P. Hill, V. N. Kulkarni, and R. L. Greene, *Phys. Rev. Lett.* **92**, 167001 (2004).
 - [8] P. Li, F. F. Balakirev, and R. L. Greene, *Phys. Rev. Lett.* **99**, 047003 (2007).
 - [9] L. B. Rigal, D. C. Schmadel, H. D. Drew, B. Maierov, E. Osquiguil, J. S. Preston, R. Hughes, and G. D. Gu, *Phys. Rev. Lett.* **93**, 137002 (2004).
 - [10] L. Shi, D. Schmadel, H. D. Drew, I. Tsukada, and Y. Ando,

- cond-mat/0510794 (2005).
- [11] A. Zimmers, L. Shi, D. C. Schmadel, W. M. Fisher, R. L. Greene, H. D. Drew, M. Houseknecht, G. Acbas, M.-H. Kim, M.-H. Yang, et al., Phys. Rev. B **76**, 064515 (2007).
- [12] J. Lin and A. Millis, Phys. Rev. B **72**, 214506 (2005).
- [13] S. Chakravarty and H.-Y. Kee, cond-mat/0710.0608 (2007).
- [14] A. Millis and M. Norman, cond-mat/0709.0106 (2007).
- [15] T. D. Stanescu and G. Kotliar, Phys. Rev. B **74**, 125110 (2007).
- [16] T. D. Stanescu, P. Phillips, and T. P. Choy, Phys. Rev. B **75**, 104503 (2007).
- [17] M. Civelli, M. Capone, A. Georges, K. Haule, O. Parcollet, T. D. Stanescu, and G. Kotliar, Phys. Rev. Lett. **100**, 046402 (2008).
- [18] J. M. Luttinger, Phys. Rev. B **84**, 814 (1951).
- [19] L. M. Roth, J. Phys. Chem. Solids **23**, 433 (1962).
- [20] T. Kita and M. Arai, J. Phys. Soc. Jpn. **74**, 2813 (2005).
- [21] N. Harrison, R. McDonald, and J. Singleton, arXiv:0708.2924 (2007).